

Analysis and Design of a Lighter-than-Air Vehicle with an Internal Vacuum

Analysis and Design of a Lighter-than-Air Vehicle with an Internal Vacuum

Edited by

Anthony Palazotto

Cambridge
Scholars
Publishing



Analysis and Design of a Lighter-than-Air Vehicle
with an Internal Vacuum

Edited by Anthony Palazotto

This book first published 2024

Cambridge Scholars Publishing

Lady Stephenson Library, Newcastle upon Tyne, NE6 2PA, UK

British Library Cataloguing in Publication Data

A catalogue record for this book is available from the British Library

Copyright © 2024 by Anthony Palazotto and contributors

All rights for this book reserved. No part of this book may be reproduced, stored in a retrieval system, or transmitted, in any form or by any means, electronic, mechanical, photocopying, recording or otherwise, without the prior permission of the copyright owner.

ISBN (10): 1-0364-0370-X

ISBN (13): 978-1-0364-0370-6

This book is a compilation of nine technical archival publications describing the analysis of various Icosahedrons primarily of a nonlinear nature. Static and dynamic characteristics are considered. The topics covered range from large displacements and rotations to the consideration of chaotic behaviour. There is a great deal of experimentation included in several papers both from a quasi- static point of view as well as that of dynamics.

Chapter One

Adorno-Rodriquez, R., Palazotto, A., “Nonlinear Structural Analysis of an Icosahedron Under an Internal Vacuum”, AIAA, Journal of Aircraft, Vol.52, No.3, May-June,2015, pp 878-883.

Chapter Two

Just, L., Deluca, A., and Palazotto, A.,” Nonlinear Dynamic Analysis of an Icosahedron Frame Which Exhibits Chaotic Behavior”, ASME, Journal of Computational and Nonlinear Dynamics”, January, 2017, pp 011006-1-10.

Chapter Three

Cranston, B., AlGhofaily, M., and Palazotto, A., “Design and Structural Analysis of Unique Structures Under an Internal Vacuum”, Aerospace Science and Technology, Vol. 68, 2017, pp 68-76.

Chapter Four

Snyder, J, and Palazotto, A., “Finite Element Design and Modal Analysis of a Hexakis Icosahedron Frame for Use in a Vacuum Lighter -than -Air Vehicle”, ASCE, Journal of Engineering Mechanics Vol. 144 No. 6, 2018, pp 04018042-1-7.

Chapter Five

Metlen, T., Palazotto, A., and Cranston, B., “Economic Optimization of Cargo Airship”, CEA Aeronautical Journal, Vol. 7, No. 2, 2016, pp 287-298.

Chapter Six

Graves, D., Moore, K., and Palazotto, A., “Analysis of a Celestial Icosahedron Shaped Vacuum Lighter-than-Air Vehicle”, Aerospace Science and Technology, Vol. 95, 2019, pp 105344-1-7.

Chapter Seven

Adorno, R., and Palazotto, A., “Evaluation of and Air-Stiffened Toroidal Sphere Subjected to Pressure”, AIAA Journal, Vol. 59, No. 1, January, 2021, pp 1-6.

Chapter Eight

Adorno, R., and Palazotto, A., “A Finite Element Study on the Effects of Thickness and Material Nonlinearity on the Equilibrium Path of Axially Loaded Circular Cylindrical Shells”, *Engineering Structures*, Vol. 277, 2023, pp 11544-1-8.

Chapter Nine

Quick, T., and Palazotto, A., “Analysis of Celestial Icosahedron”, *ASCE, Journal of Engineering Mechanics*, Vol. 148, No. 1, 2022, pp 06021006-1 -7.

CONTENTS

| | |
|--|-----|
| Chapter One..... | 1 |
| Nonlinear Structural Analysis of an Icosahedron under an Internal Vacuum | |
| <i>Ruben Adorno-Rodriguez and Anthony N. Palazotto</i> | |
| Chapter Two | 20 |
| Nonlinear Dynamic Analysis of an Icosahedron Frame | |
| that Exhibits Chaotic Behavior | |
| <i>Lucas W. Just, Anthony M. Deluca and Anthony N. Palazotto</i> | |
| Chapter Three | 46 |
| Design and Structural Analysis of Unique Structures | |
| under an Internal Vacuum | |
| <i>Brian Cranston, Mohammed AlGhofaily, Captain, RSAF</i> | |
| <i>and Anthony Palazotto</i> | |
| Chapter Four..... | 69 |
| Finite Element Design and Modal Analysis of a Hexakis Icosahedron | |
| Frame for Use in a Vacuum Lighter-Than-Air Vehicle | |
| <i>Jordan W. Snyder and Anthony Palazotto</i> | |
| Chapter Five | 88 |
| Economic Optimization of Cargo Airframe Trent Metlen | |
| <i>Anthony Palazotto and Brian Cranston</i> | |
| Chapter Six | 115 |
| Analysis of a Celestial Icosahedron Shaped Vacuum | |
| Lighter than Air Vehicle | |
| <i>Dustin P. Graves, Kyle D. Moore and Anthony N. Palazotto</i> | |
| Chapter Seven..... | 138 |
| Evaluation of an Air-Stiffened Toroidal Sphere Subjected to Pressure | |
| <i>Ruben Adorno and Anthony N. Palazotto</i> | |

| | |
|--|-----|
| Chapter Eight..... | 155 |
| A Finite Element Study on the Effects of Thickness and Material Nonlinearity on the Equilibrium Path of Axially Loaded Circular Cylindrical Shells <i>Ruben Adorno and Anthony N. Palazotto</i> | |
| Chapter Nine..... | 175 |
| The Analysis of a Celestial Icosahedron <i>Torin Quick and Anthony Palazotto</i> | |

CHAPTER ONE

NONLINEAR STRUCTURAL ANALYSIS OF AN ICOSAHEDRON UNDER AN INTERNAL VACUUM

RUBEN ADORNO-RODRIGUEZ
AND ANTHONY N. PALAZOTTO

Air Force Institute of Technology, WPAFB, Ohio, 45433

The concept that a structure is capable of producing buoyancy using an internal vacuum rather than a gas dates back to the 1600s; but material technology has restricted the construction of such concepts for common geometries, such as the sphere. Different and often complex geometries compensate for the lack of light materials that provide the stiffness and strength needed. Therefore, this research looks at a Lighter than Air Vehicle (LTAV) in the form of an icosahedral frame/skin configuration using nonlinear finite element analysis in order to determine the structural response of such a vehicle, its capacity to sustain a vacuum with both material technology that exists today and in the near future, and its buoyancy characteristics. The structural response is characterized with large displacements; where membrane behavior dominates the icosahedral skin response, generating geometric stiffening in the overall structure. It is shown that those displacements have minimal effect in the structure's buoyancy, with no more than 4% reduction. Overall, the nonlinear analysis of the icosahedral structure provided tangible background on its behavior and the LTAV applicability. It is feasibly possible to actually manufacture this type of vehicle in the very near future depending upon newer materials with more advanced strength.

Nomenclature

W = weight of structure

ρ = density

V_{frame}, V_{skin} = frame and skin volume respectively

1. Introduction

Aircraft structures have been designed for more than a century with wing like configurations; tremendous progress has been made in this direction. The research presented in this paper is an attempt to evaluate a different type of air structure: a structure that relies on the effect of buoyancy through an internal vacuum to provide lift rather than the normal wing. Therefore, the objective is to evaluate the characteristics of LTAV subjected to a vacuum, pointing out the structural features for consideration in the eventual design of such a vehicle.

In order to evaluate the vacuum, Archimedes principle with the ideal gas law along with nonlinear FEA with the Newton Raphson technique is used. The Archimedes principle states that an object submerged in any fluid exerts a buoyant force equal to the weight of the displaced fluid, establishing the relationship that allows the design to become lighter than Air. Furthermore, the ideal gas law serves to express the air density in terms of pressure and altitude, providing a direct relationship between the atmospheric pressure and the pressure acting on the structure. FEA then provides the means to evaluate the nonlinear behavior of the structure and its relationship to buoyancy.

A historical question arises: 'Why, after so many years of development, did the dirigibles vanish (for the most part)?' Dirigibles had major challenges over those years, including their speed and control limitations, safety and poor ground handling qualities. The advancements of heavier than air vehicles during that period were the main reason for the disappearance of dirigibles. Furthermore, airplanes eliminated most of the safety and handling issues. Safety mostly relates through history with the use of hydrogen as a lifting gas. Being flammable, hydrogen has been reported to be the cause of more than 22 accidents related to dirigibles from 1930 to 1937. Helium, on the other hand, is an inert gas and therefore it has been used since 1960s in dirigibles, but it being a depleting nonrenewable energy source, has created restraint in LTAV designs throughout the years.

In the last decade, technology has driven new, safer and efficient LTAV designs. The Lockheed P-791 hybrid air vehicle, having its first flight on January, 2010 is an example of these designs. Hybrid designs take advantage of aerodynamics in combination to its buoyancy to produce lift and movement. These designs have solved most of the safety and ground handling issues that previous dirigibles had, but they still rely on Helium as the lifting gas.

In the same way, today's advantages in materials and manufacturing techniques makes producing buoyancy by evacuating a structure (creating a vacuum inside) an idea that is not as far-fetched as when Lana [1] suggested it. He suggested the use of vacuum spheres. The sphere is the ideal shape for a vacuum LTAV since it achieves the greatest stiffness with the least weight, therefore maximizing buoyancy. The result of this is a material that has enough specific stiffness, $(E^{1/2} / \rho)$ where E is the modulus of elasticity and ρ is the density. If $E^{1/2} / \rho$ is used to minimize weight while maximizing stiffness, a homogeneous sphere has not been found to capture buoyancy with an internal vacuum. Therefore, designers have resorted to other geometries to compensate for the lack of material stiffness. Two of the LTAV designs found in published literature that use an internal vacuum are mentioned here. First, A. Akhmeteli and A.V. Gavrilin [2] proposed the use of layered shell spheres, a sandwich construction type, and second, T.T. Metlen [3] considered the icosahedron and rotating cylinders.

From the structural point of view, a LTAV requires an internal vacuum, and thus a rigid design is needed since there is no internal gas to force it into shape. Imagine a simple balloon: inflating it with helium would cause it to float; since the air displaced weighs more than the balloon and helium themselves. However, if the helium is vacated out of the balloon, the balloon would shrink and no internal volume will be left, such that the balloon becomes heavier than air. On the other hand, a rigid structure, or a rigid balloon for that matter, can maintain its internal volume once vacated, provided it is stiff enough to resist the external forces.

The research presented in this paper tries to answer questions that arise from Metlen's research by evaluating the icosahedral structure with nonlinear analysis. The geometric characteristics of the icosahedron are presented next to provide background on the reasoning of selecting such geometry.

2. The Icosahedron as a Geometrical Shape

The icosahedron, properly called a regular icosahedron, is a regular polyhedron and platonic solid. The word 'regular' refers to polygons that are characterized by sides of the same size, located symmetrically about a common center, such as the equilateral triangle and the square. A polyhedron is then regular if its faces and vertex figures are regular. Furthermore, a platonic solid is a convex polyhedron (that can be algebraically defined as the set of solutions to a system of linear inequalities) with equivalent faces composed of regular polygons.

The icosahedron has advantages that revolve around one characteristic: symmetry which leads to a simple construction. Symmetry results from the 20 equilateral triangles that form the icosahedron. The icosahedron and its decomposition into 20 triangles are shown in figure1. As a symmetry byproduct, a circumscribed sphere touches each of the 12 vertices that make the icosahedron, such that an icosahedral radius is defined as the distance from the center to each vertex. From the structural point of view, symmetry provides many advantages including uniform stress distribution, simplified construction (compared to other polyhedrons) and modeling simplifications. The latter becomes important since a simplified structure can yield an accurate model. One of the modeling simplifications is the use of one triangle to approximate the behavior of the structure, done with the triangle submodule. A great deal of convergence evaluation was carried out as detailed in reference [4].

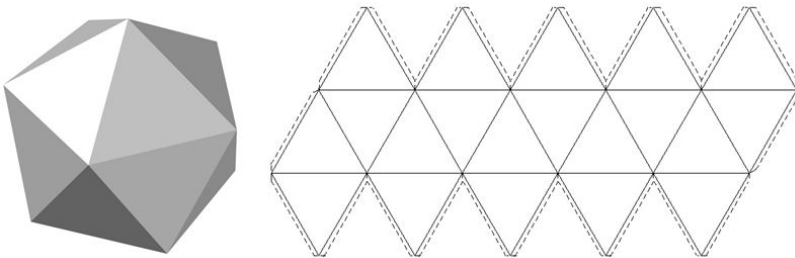


Figure 1: Icosahedron, left. Three- dimensional shape, right: planar decomposition

3. Analysis and Modeling

The evaluation of an icosahedron is presented in this section. Reference [4] presents all of the appropriate details and should be consulted for

specific facts. This section will be limited to some appropriate features of the analysis. The weight to buoyancy ratio W/B is looked at first. It is a concept that establishes how buoyant (free to float) a structure is with respect to its own weight. In an ideal situation, this ratio is close to zero such that its weight is much less than its buoyant force producing lift in this case the icosahedron is subjected to a vacuum.

We have two main components, the frame and the skin, as shown in Figure 2. The icosahedron W/B is

$$\frac{W}{B} = \frac{V_{skin}\rho_{skin} + V_{frame}\rho_{frame} + (V_i - V_r)\rho_{air,i}}{(V_i - V_r)\rho_{air,o}} \quad (1)$$

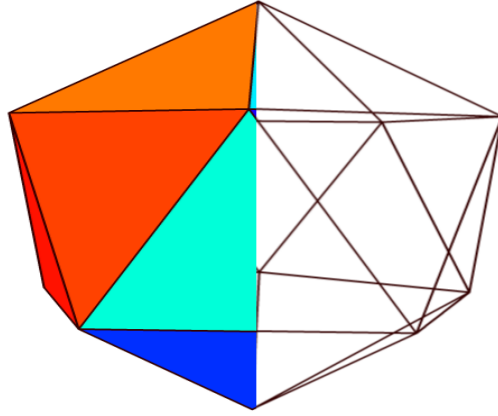


Figure 2: Icosahedral Frame/Skin Combination – skin (left half), frame (right half)

Where V_{frame}, V_{skin} = frame and skin volume respectively

V_i = icosahedron internal volume before deformation

V_r = icosahedron internal volume reduction

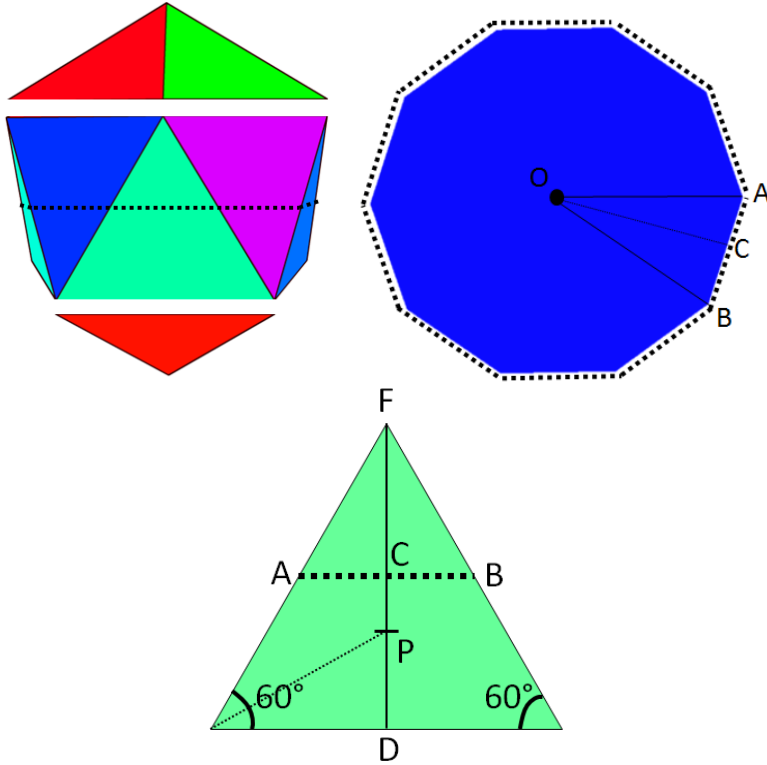
W = weight of the structure,

$\rho_{air,i}, \rho_{air,o}, \rho_{frame}, \rho_{skin}$ = internal, external, frame, skin density respectively

Considering the icosahedron volume, one should note that a circumscribed sphere touches each of the vertices, such that the radius, r , is measured from the center to any vertex. In addition, an inscribed sphere with radius, r_i , touches each triangle at the centroid. Next, consider a mid-plane

perpendicular to an imaginary line drawn in between opposite vertices, extracted from Figure 3a and shown in Figure 3b by the dotted line, where A and B are two vertices on the mid-plane, as shown in Figure 3c. Then, $r = OA = OB$, where O is the icosahedron center. The center cutout shown in Figure 3a has 10 faces around, therefore the angle OAB is

$$OC = AC \cos 18^\circ = BC \cot 18^\circ \quad (2)$$



(a) Partition

(c) Equilateral Triangle

(b) Mid-plane

Figure 3: Icosahedron Decomposition

Further geometric determination can be found in [4]. Once the altitude is selected for evaluation and the W/B ratio chosen, the actual thickness of the skin and the size of the stiffeners making up the frame can be evaluated. Sea level was chosen for the analysis elevation and the sea level pressure equals 101.25 kPa and has a density of 1.2041 kg/m^3 . The frame was made up of circular tubes joined together at their ends. Again [4] shows a great deal of information related to the various convergence studies carried out and the results related to the optimized frame geometry makeup. The analysis was almost entirely nonlinear and for that Abaqus was used. The program has the capability of allowing normal pressure to act on a membrane using the technique of adaptive automatic stabilization. Adaptive automatic stabilization was necessary to allow the membrane to resist transverse pressure. It was found that without this technique the membrane had to be modeled with a very thin plate element. The asymmetric matrix storage was needed to adjust the solution to the necessary follower force brought about by the pressure.

One of the main features of the icosahedron is symmetry. This property provides several structural advantages such as equal surface loading, improved stress distribution and buckling retardation. Additionally, the actual design will have no BC once afloat. The FEA requires the model to have a BC since otherwise the static analysis runs into gross inaccuracies. Therefore, it is important to select them such that symmetry is maintained throughout the analysis. Three BCs were considered. The first has the bottom vertex fixed therefore all six DOF are constrained. The second has the bottom vertex fixed and the top vertex with the DOF 1 and 2 constrained. The third has both bottom and top vertices with only DOF 1 and 2 constrained. The third BC is shown in Figure 4. This is the BC which led to symmetry of movement.

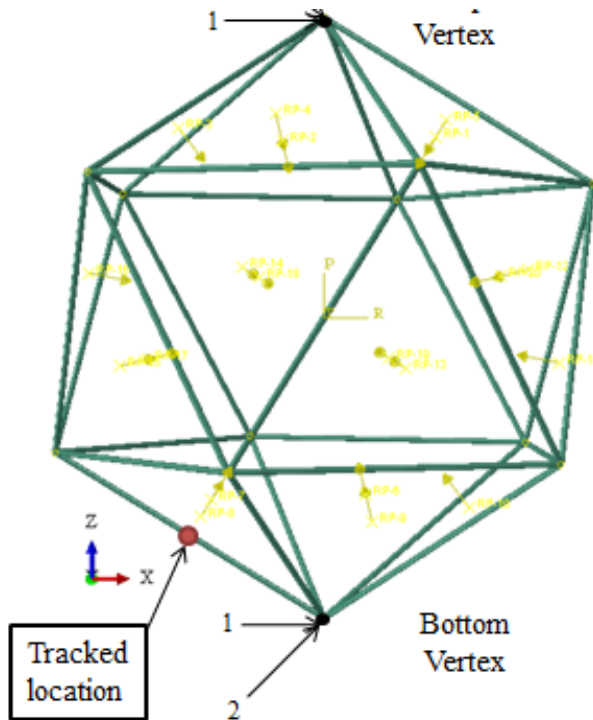


Figure 4: BC 3

4. Models and Results

The basic model is a conglomerate of previously stated techniques and design features. The following modeling techniques and properties are shared in all icosahedral models considered for analysis:

- Dimensionality: A fixed diameter of 0.3048 m (1 ft.) was selected, with a beam thickness to radius ratio, c , and equal to 0.05. The beam radii and skin thicknesses were derived for a desired W/B .
- Load: the load was set at SL pressure (101,325 Pa).
- Boundary Conditions: the BC that produced symmetry was selected (BC 3 in Figure 4). The symmetric BC was composed by fixing the displacements: $U1=U2=0$, of opposite vertices. The arrows displayed in this figure represent how a radial force is applied at a reference point which is then distributed to the frame.

- Mesh: the mesh was composed of M3D3 membrane elements for the skin and B32 beam elements for the frame.
- Analysis: the Newton Raphson technique with adaptive automatic stabilization was selected along with asymmetric matrix storage. Also, solution controls within the Abaqus algorithm, were adjusted to aid convergence. A linear buckling analysis was conducted in one of the models in order to visualize buckling mode shapes [4].
- Constraint: the tie constraint was used to connect the skin to the frame by only tying the displacement DOF.

A representation of the basic model is shown in Figure 5, where arrows represent the radial acting pressure applied to the skin. Note how the skin is tied at the mid-plane of beams, such that half of the beam cross-sections are exposed. Using the basic model, seven particular models were developed by changing the material properties and desired W/B. Material properties related to three materials were selected, as shown in Table 1: The materials chosen were Beryllium, Spectra, and Carbon Nanotubes. The research was only interested in the properties of the materials with no real interest in their availability for actual manufacturing purposes since the effort was directed to see if a structure can float with an internal vacuum. Beryllium is a metal used in light weight components of military equipment. It is the only one of the three looked at that has any practical manufacturing application. Spectra is a fiber of high strength. Carbon Nanotubes (CNT) is an arrangement of carbon atoms that have been rolled into a tube. One may find a great deal of information about each on the internet. Table 1 indicates how each material was distributed between the membrane and the frame for the various models. The models numbers indicating the various combinations. Material #5 was selected because, though still in research, provides the best combination of specific stiffness and strength. On the other hand, material # 6 is the weakest of the three selected, but is a material well researched, with linear behavior with commercially available. Material # 10 provides a middle ground between the other two in terms of strength and stiffness. Materials and buoyancy (W/B) of models developed are shown in Table 1. Note in Table 1 that the first five models have a desired W/B of 0.9, while the first three have the material properties of selected materials for both skin and frame. Models 4 and 5 are composed of hybrid combinations of Beryllium and Spectra fiber frames with CNT skin, respectively; thus providing stiffened versions of models 1 and 2, respectively.

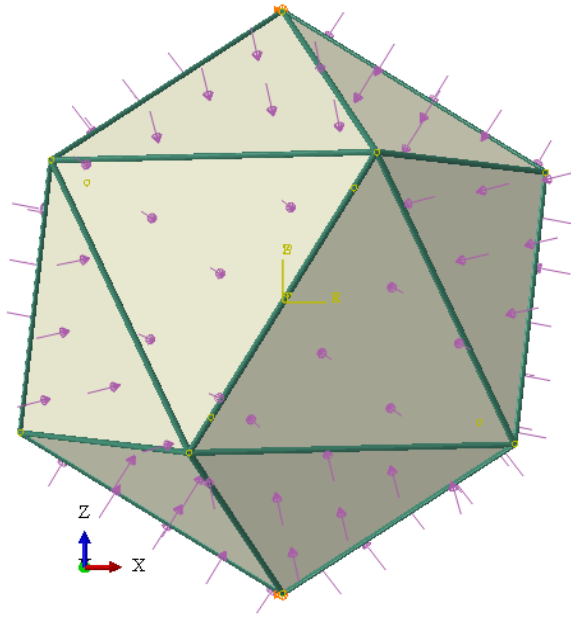


Figure 5: Basic Model with the Applied Pressure Shown

Once the model has been evaluated, the results of loading on the seven models will be considered. The effect of structural deflection on the W/B depends on two factors: volume reduction and applied pressure. Applied pressure versus W/B are plotted in Figure 6, with the full range of pressures at the bottom and the range pressures that provide a $W/B \leq 1$ at the top. In regards to the effect on volume reduction at the feasible vacuum, note that models exhibit a W/B equal to the desired W/B (0.9 for Models 1 to 5, 0.8 for Models 6 and 7; (see Table 1) minus the volume reduction for each model. Note that relatively linear behavior is seen in the W/B curves, as a result of the linear behavior of volume reduction. It should be noted that all models are buoyant at the range of applied pressures shown in Figure 6.

Table 1 Icosahedron models

| Model | Materials | | Desired W/B | | r_{beam} | t_{skin} |
|--------------|---------------|--------------|-------------|------|-------------------|-------------------|
| | Frame | Skin | Frame | Skin | | |
| No. Elements | | | | | | |
| 1 | 6 (beryllium) | 6(beryllium) | 0.5 | 0.4 | 1.41E-03 | 1.05E-05 |
| 7020 | | | | | | |
| 2 | 10 (Spectra) | 10 (Spectra) | 0.5 | 0.4 | 1.95E-03 | 2.00E-05 |
| 8500 | | | | | | |
| 3 | 5(CNT) | 5 (CNT) | 0.5 | 0.4 | 1.49E-03 | 1.18E-05 |
| 7020 | | | | | | |
| 4 | 6 (beryllium) | 5 (CNT) | 0.5 | 0.4 | 1.41E-03 | 1.18E-05 |
| 7020 | | | | | | |
| 5 | 10 (Spectra) | 5 (CNT) | 0.5 | 0.4 | 1.95E-03 | 1.18E-05 |
| 8600 | | | | | | |
| 6 | 10 (Spectra) | 10 (Spectra) | 0.4 | 0.4 | 1.74E-03 | 2.00E-05 |
| 7020 | | | | | | |
| 7 | 5(CNT) | 5 (CNT) | 0.4 | 0.4 | 1.33E-03 | 1.18E-05 |
| 8600 | | | | | | |

Once buoyancy effects are established and symmetry is verified for all models, only critical points on the design are considered to represent the structural response of icosahedron models. These critical points are; the displacement at a vertex, the edge midpoint displacement and the displacements at the triangle's center. Since both frame and skin share nodes along edges, a vertex and a midpoint represent the behavior of both parts along the edges. First, the applied pressure versus vertex displacement is plotted in Figure 7 and considered for all seven models. The displacement is normalized by the beam diameter of each model. The dashed horizontal line is the feasible vacuum line. The horizontal-colored lines represent the points at which each model achieves neutral buoyancy ($W/B = 1$). Note, for example, that models 6 and 7 achieve neutral buoyancy before the first five models. That is because the desired W/B of these models was 0.8, instead of 0.9; and as seen in Figure 6, the W/B does not change considerably. Regardless, color lines represent the 'true' W/B (including the volume reduction). Note that a closely linear relationship is observed for the vertices of all seven models, with deflections in the order of 0.15 to 0.7 times their respective beam diameters. As expected, these displacements are not as pronounced in stiffer models (3 and 7). The slope difference between models 1 and 3 is as

much as 114%, a definite proof of how much the material stiffness contributes to the overall behavior of the structure.

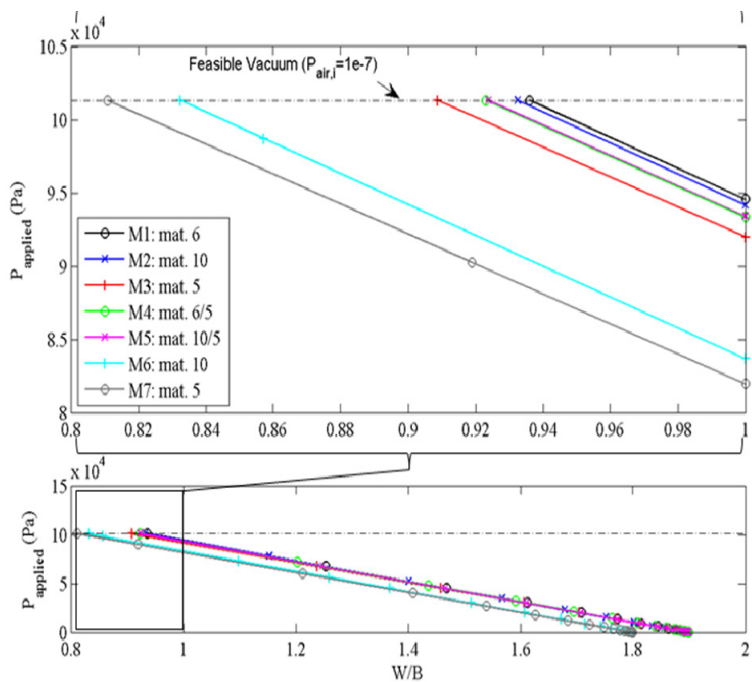


Figure 6: Icosahedron –Applied Pressure Versus W/B Bottom Close up for $W/B \leq 1$

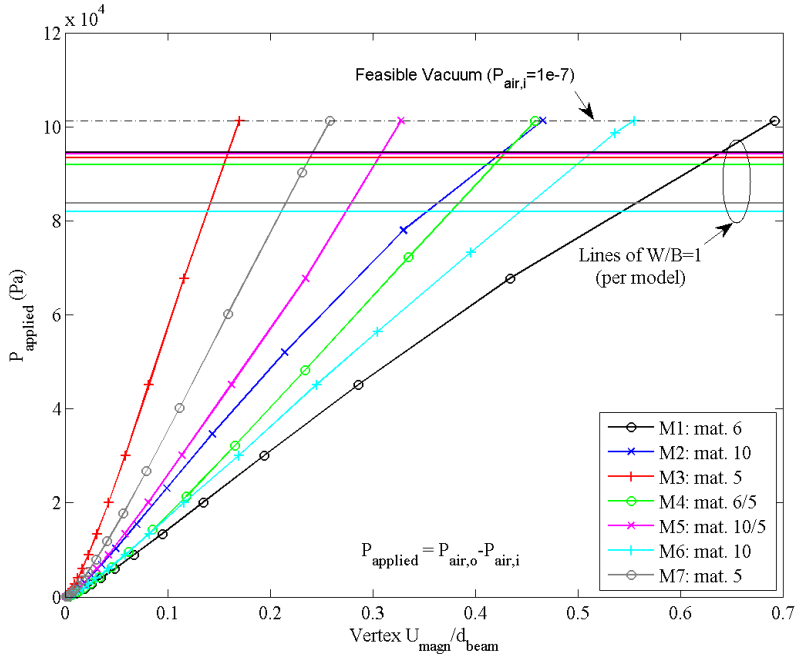


Figure 7: Applied Pressures versus Vertex Displacement Normalized by the Beams Diameter

The next critical point is a triangular face center. The face center deflection, normalized by skin thickness as applied pressure increases, is shown in Figure 8 for all models. Observe the nonlinearity in the entirety of the curves. The skin initially displaces considerably in the lower left corner, up to 200 times the skin thicknesses. This behavior is consistent with a membrane. Since there is no bending stiffness, the skin is required to deflect in order to acquire membrane stiffness. The slope starts increasing significantly in all models after 200 times the thicknesses, a clear sign of a continuous increment in membrane forces. Stiffening occurs as a result. Note the difference in slopes between model 1, the less stiff model, and model 2. It is clear that specific stiffness does play an important role in the overall stiffness of the structure, a desired result that minimizes buoyancy loss. When comparing models 2 and 3, a stiffer response would be expected in Model 3 since it is materially stiffer. But the density of model 2 is about 40% less, thus the skin thickness increases considerably for a desired W/B, ergo producing significant geometric

stiffness that result in similar responses. These large deflections bring a numerical concern, the possibility of element distortion, which usually results in loss of accuracy. Therefore, the mesh was verified and no distortion was found; and the latter is believed to be a result of the mesh uniformity along the whole icosahedral structure.

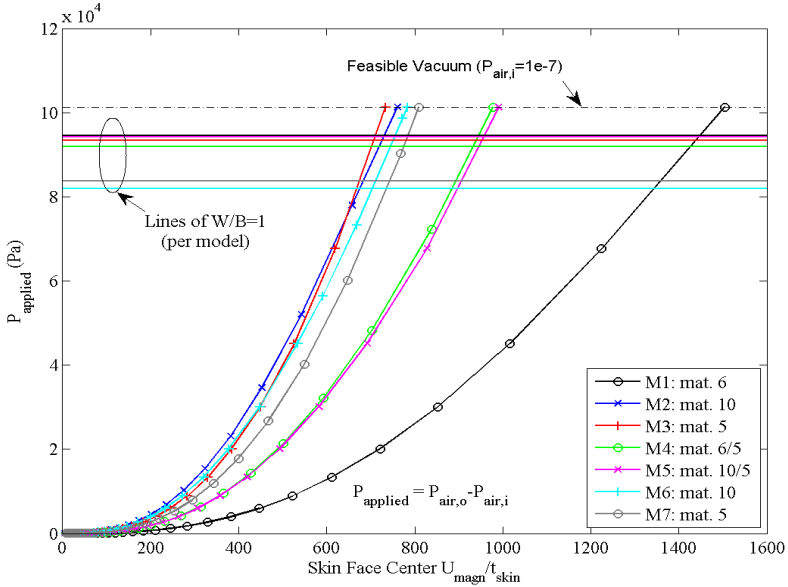


Figure 8: Applied Pressures versus Normalized Skin Center Displacement

Nonlinear static analysis provided great insight on the structural response of the icosahedron. First, the volume reduction resulting from the skin deflection proved to be minimal, causing minimal effect on the W/B of the different models with the largest reduction being 0.04; consistent with what was found in the single triangle study. Second, large displacements were found in all the parts of the icosahedron model, the least occurring at vertices, followed by edge midpoints, and the largest occurring at face centers. Regardless, all models remained stable during the entire analysis, with significant hardening occurring in the skin that helped increase overall model's stiffness. Third, since the analysis was carried out using elastic material properties, vertices presented a singularity of stress within the membrane. The value of the von Mises stress that exceed yield was traced from the vertex for each model and found to exist over a distance of

5% of the beam length for all of the models except Model 3 and 7 both made entirely of CNT. This suggests that stiffening those areas not only will prevent numerical failure, but it would make model 7 feasible. Subsequent research has shown that it is possible to remove this elastic failure by designing a structure slightly different than the discussed icosahedron or considering the elastic plastic nature of some of the materials. Neither of these solutions is presented within this paper. Results for models 3 and 7 are summarized in Table 2, including maximum displacements and stresses for frame and skin, the W/B and the maximum altitude. The maximum altitude is predicated on the fact that an ultra high vacuum is used. The safety factors are calculated using the estimated yielding point.

Table 2 Feasible Models

| Models | | | |
|---|-----------|-----------|---|
| r_{beam} (mm) | 1.49 | 1.33 | 7 |
| t_{skin} (mm) | 0.0118 | 0.0118 | |
| W/B | 0.91 | 0.81 | |
| Maximum Altitude - with Ultra High Vacuum (m: ft) | 512; 1680 | 676; 2219 | |
| Material Properties | | | |
| Density (kg/m^3) | 1650 | 1650 | |
| Poisson's ratio | 0.2 | 0.2 | |
| Modulus of Elasticity (GPa) | 1000 | 1000 | |
| Frame | | | |
| Maximum Displacement (mm) | 3.05 | 3.97 | |
| Maximum von Mises Stress (Pa) | 6.79E+09 | 8.64E+09 | |
| Safety Factor | 1.47 | 1.16 | |

Skin

| | | |
|---|----------|----------|
| Maximum Displacement (mm) | 8.64 | 9.53 |
| Maximum von Mises Stress (Pa) | 9.62E+09 | 1.33E+10 |
| Safety Factor (w.r.t the yielding point) | 1.04 | 0.75 |
| Maximum von Mises Stress - No Singularities (Pa) | 5.15E+09 | 5.83E+09 |
| Safety Factor - No Singularities (w.r.t the yielding point) | 1.94 | 1.72 |

5. Conclusions

The conclusions presented are considered for design only.

(a) The selection of an appropriate cross-section for the frame members greatly influences the stiffness and failure modes of the entire structure. The study showed that for beams of circular cross-section, the performance improves in exponential fashion as the thickness of the beams tends to 0. Therefore, manufacturability and material selection need to be considered in order to attain an improved performance.

(b) The material selection becomes the critical design factor for LTAV subjected to a vacuum. Preliminary studies show that the response is highly dependent on the specific stiffness, therefore the modulus of elasticity and density become the driving constraints with minimal stiffness effects from changes in the Poisson's ratio. The response of the icosahedron shows that, due to elastic consideration, stress exceeds the yield at or near the vertices for some models indicating the need for high specific strength in order to sustain the high stress levels that result from thin components.

(c) The membrane forces in the icosahedral skin provide significant stiffness to the overall structure. The skin shows significant hardening as a byproduct of the large deflections.

(d) The frame provides structural stability, allowing for the structure to sustain large deflections without collapsing.

Acknowledgment

The authors would like to thank Dr. David Stargel of AFOSR for his financial support and encouragement. The views expressed in this work are those of the authors and do not reflect the official policy or position of the United States Air Force, the Department of Defense, or the U.S. Government. The material is declared a work of the U.S. Government and is not subject to copyright protection in the United States.

References

- [1] Lana-Tergi, F., “The Aerial Ship”, The Aeronautical Society of Great Briton, 1910
- [2] Akhmeteli, A., and Gavriln, A., “Layered Shell Vacuum Balloons”, Patent application, May, 2005, URL <http://akhmeteli.org/lighter-then-air-solid>
- [3] Metlen, T., “Design of a Lighter than Air Vehicle that 3Achieves Positive Buoyancy in Air Using a Vacuum”, MS Thesis, Air Force Institute of Technology, June, 2013.
- [4] Ruben Adorno-Rodriguez, “Nonlinear Structural Analysis of an Icosahedron and Its Application to Lighter Than Air Vehicles Under a Vacuum “, MS Thesis, Air Force Institute of Technology, March, 2014

CHAPTER TWO

NONLINEAR DYNAMIC ANALYSIS OF AN ICOSAHEDRON FRAME THAT EXHIBITS CHAOTIC BEHAVIOR

LUCAS W. JUST, ANTHONY M. DELUCA
AND ANTHONY N. PALAZOTTO

Air Force Institute of Technology, WPAFB, OH, 45433

The overall problem that has been considered is to develop an icosahedron that can make use of an internal vacuum to become positively buoyant. In order to create this vacuum, it is necessary to evacuate internal gas, thus creating a dynamic effect on the supporting frame which makes up the structure. This paper considers the frame of an icosahedron under **external atmospheric pressure**. It has been found that a static finite element analysis generated a *snapback* phenomenon for certain boundary **support conditions**. When the dynamic analysis under the same boundary conditions was considered, a chaotic behavior resulted. Thus, the various chaotic responses for a given **set** of boundary conditions are determined. The entire analysis is carried out nonlinearly in which a method relying on a reference point distribution of external pressure is incorporated in distributing the external pressure. A method of combining the power spectral density and the Lyapunov exponent has been followed to yield the formulated outcome.

Nomenclature

R^{int} = internal force BC = boundary condition
 D, \dot{D}, \ddot{D} = displacement, velocity, and acceleration vectors, respectively
 DoF = degree of freedom
 FEA = finite element analysis

| | | |
|---------------|---|--|
| K, k | = | stiffness matrix and individual stiffness |
| L_p | = | length between two points in reconstructed attractor |
| L_p' | = | evolved length between two points in reconstructed attractor |
| LTAV | = | lighter than air vehicle |
| M, m | = | mass matrix and individual mass |
| N | = | number of replacement points |
| PSD | = | power spectral density |
| R^{ext} | = | externally applied load vector |
| vector | | |
| R_x | = | autocorrelation function |
| S_x | = | power spectral density function |
| r | = | ramp input function |
| \mathcal{r} | = | ramp response function |
| s | = | step response function |
| t | = | time |
| u | = | step input function |
| λ_1 | = | Lyapunov exponent |
| τ | = | time delay |
| ω | = | frequency |

1. Introduction

The Air Force Instituted of Technology has been studying a lighter than air vehicle (LTAV) in the shape of an icosahedron, which is made up of a frame consisting of 12 vertices, 20 equilateral triangles, and 30 beams. The unique feature to this study is the fact that the internal gas usually associated with a LTAV is removed and a vacuum is assumed to exist. Thus, the frame of the vehicle becomes the main supporting device and the need for a structural dynamic analysis of the frame is required. Metlen [1] and Rodriguez [2] have carried out the frame static analysis utilizing Abaqus Finite Element Analysis (FEA) software and found, under certain conditions, the beam components showed nonlinear *snapback*. The present analysis carried the work forward by considering a nonlinear dynamic analysis of the same frame by evacuating the internal air as a function of time. The interesting feature to this study is the fact that chaotic behavior resulted in the frame [2].

2. Background

While the concept of using a vacuum to achieve positive buoyancy is centuries old, the idea of using an icosahedron frame with a membrane-like

skin as a structure is relatively new. The idea was originally conceived by Trent Metlen of the Air Force Institute of Technology in 2013 [1]. An icosahedron is made up of twenty equilateral triangles formed into a shape that has 12 vertices, each of which lies on an encompassing sphere. The nearly spherical shape is an important feature because a sphere is the ideal geometric shape when considering a structure that can achieve positive buoyancy using an inner vacuum, as it displaces the greatest volume per surface area. The structure is also geometrically symmetric so that each of the members of the frame carries an equally distributed load, and the stress within those members is equal.

Following Metlen's research, Ruben Adorno-Rodriguez developed a FEA model to analyze the icosahedron shaped LTAV, and conducted a static structural analysis on the design [2]. Figure 1 shows the structure with the boundary conditions and the loading applied to the icosahedron frame that Adorno-Rodriguez analyzed. The loads are applied through reference points at the center of gravity of each triangle, which is distributed to the beams using a coupling constraint in Abaqus. The coupling constraint allows the beams to experience an equivalent load to one that would be applied if a triangular skin with an applied pressure was tied along the edges. Adorno-Rodriguez conducted a study to ensure the applied load experienced by the beams was identical using the reference point and coupling constraint method, or using a skin tied to the beams [2]. The midpoint node on the lower beam is where all displacement data is collected. The midpoint node was used because the icosahedron deforms symmetrically, and all midpoint nodes on all beams have equivalent displacement. Also, it has the greatest displacement of any node on the structure. The boundary conditions that are applied to the structure in Figure 1 allow the frame to displace symmetrically, and move freely in the z-axis as the structure would if it were floating. The lack of a z-axis boundary condition does not result in rigid body movement because the structure is symmetric and the load applied to the bottom half is equivalent to the load applied in the top half of the structure resulting in an equilibrium state. However, the x (U1) and y (U2) degrees-of-freedom (DoF) at the top and bottom node are constrained in order to prevent rigid body movement in the x-y plane and allow the FEA software to converge on a solution. The boundary conditions applied in Figure 1 are referenced as Boundary Condition 3 (BC3) in the previous research, and the notation is preserved in this research. The dimensionality and the material properties used for the frame are listed in Table 1.